

Correlation function for generalized Pólya urns: Finite-size scaling analysis

Shintaro Mori*

Department of Physics, Kitasato University

Kitasato 1-15-1, Sagamihara, Kanagawa 252-0373, JAPAN

Masato Hisakado

Financial Services Agency

Kasumigaseki 3-2-1, Chiyoda-ku,

Tokyo 100-8967, Japan

(Dated: November 9, 2015)

Abstract

We describe a universality class for the transitions of a generalized Pólya urn by studying the asymptotic behavior of the normalized correlation function $C(t)$ using finite-size scaling analysis. $X(1), X(2), \dots$ are the successive additions of a red (blue) ball ($X(t) = 1(0)$) at stage t and $C(t) \equiv \text{Cov}(X(1), X(t+1))/\text{Var}(X(1))$. Furthermore, $z(t) = \sum_{s=1}^t X(s)/t$ represents the successive proportions of red balls in an urn to which, at the $t+1$ -th stage, a red ball is added ($X(t+1) = 1$) with probability $q(z(t)) = (\tanh[J(2z(t) - 1) + h] + 1)/2$, $J \geq 0$, and a blue ball is added ($X(t+1) = 0$) with probability $1 - q(z(t))$. A boundary $(J_c(h), h)$ exists in the (J, h) plane between a region with one stable fixed point and another region with two stable fixed points for $q(z)$. $C(t) \sim c + c' \cdot t^{l-1}$ with $c = 0 (> 0)$ for $J < J_c (J > J_c)$, and l is the (larger) value of the slope(s) of $q(z)$ at the stable fixed point(s). On the boundary $J = J_c(h)$, $C(t) \simeq c + c' \cdot (\ln t)^{-\alpha'}$ and $c = 0 (c > 0)$, $\alpha' = 1/2 (1)$ for $h = 0 (h \neq 0)$. The system shows a continuous phase transition for $h = 0$ and $C(t)$ behaves as $C(t) \simeq (\ln t)^{-\alpha'} g((1-l) \ln t)$ with a universal function $g(x)$ and a length scale $1/(1-l)$ with respect to $\ln t$. $\beta = \nu_{||} \cdot \alpha'$ holds with $\beta = 1/2$ and $\nu_{||} = 1$.

PACS numbers: 05.70.Fh, 89.65.Gh

* mori@sci.kitasato-u.ac.jp

I. INTRODUCTION

The contagion process is one of the most studied topics in statistical physics and has attracted the attention of many researchers from various disciplines [1–8]. Pólya urn is one of the simplest models for this process [9–11]. In this model, an urn consists of t balls, where the proportion of red balls is $z(t) \in (0, 1)$ and the rest of the balls are blue. The probability of a new red ball being added to the urn is $z(t)$, while it is $1 - z(t)$ for a new blue ball; the proportion of red balls then becomes $z(t+1)$. This procedure is iterative, which produces a sequence of proportions $z(t_0), z(t_0 + 1), z(t_0 + 2), \dots$, where the urn contained $t_0 \cdot z(t_0)$ red balls at $t = t_0$. The limit value $\lim_{t \rightarrow \infty} z(t)$ obeys a beta distribution with shape parameters $\alpha = t_0 \cdot z(t_0)$ and $\beta = t_0 \cdot (1 - z(t_0))$.

As the Pólya urn process is very simple and there are many reinforcement phenomena in nature and the social environment, many variants of the process have been proposed, referred to as generalized Pólya urn processes[12]. In the nonlinear generalizations of this model, a continuous function $q : [0, 1] \rightarrow [0, 1]$ determines the probability $q(z(t))$ of a red ball being added at stage $t + 1$. This nonlinear version is referred to as a nonlinear Pólya process[12–14]. In contrast to the original linear model, the nonlinear model can have many isolated stable states. The fixed point z_* of $q(z)$, where $q(z_*) = z_*$, is (un)stable if $(z - z_*)(q(z) - z)$ is negative (positive) for all z in the vicinity of z_* [13]. z_* is referred to as downcrossing (upcrossing) as the graph $y = q(z)$ crosses the curve $y = z$ in the downwards (upwards) direction. The slope of $q(z)$ at z_* is smaller (larger) than one when z_* is downcrossing (upcrossing). When $q(z)$ touches the diagonal $q = z$ in the (z, q) plane at z_t , a point that is referred to as the touchpoint, the stability of z_t depends on the difference between the slope of $q(z)$ and the diagonal z in the left neighborhood of z_t [14]. If it is less (more) than $1/2$, z_t is (un)stable. The multiplicity of the stable states provides a convenient picture that explains the lock-in phenomena in the technology and product adoption processes [15]. Suppose two selectively neutral technologies enter the market at the same time. Because economies of scale play the role of an externality that persuade a new consumer to buy the dominant technology, determining which technology to buy depends on the proportion of each technology possessed by previous consumers. If the dependence is described by the non-linear function $q(z)$, the technology adoption process is described by a non-linear Pólya urn. An S-shaped $q(z)$ function with two stable fixed points suggests the random monopoly

formed when one technology dominating over the other depends on chance fluctuations at the start [?].

Information cascade provides a good experimental setup for verifying theoretical predictions [16–19]. Here, participants sequentially answer questions with two possible choices (two-choice questions). In addition to their own information or knowledge, they refer to social information about the number of previous subjects that chose each option. In an experiment where subjects answer general knowledge two-choice questions, it is possible to change the number of stable states by controlling the difficulty of the question [18, 19]. A subject that knows the answer to a question chooses the correct answer with a probability of 1. A subject who does not know the answer tends to choose the majority choice. By changing the difficulty of the question, an experimenter can control the ratio p of the latter, no-knowledge, subject. We denote the probability that the no-knowledge subject choose the correct answer as $q_h(z)$, when the ratio of correct choices among previous subjects is z . The probability that a subject choose the correct answer is then $q(z) = (1 - p) \cdot 1 + p \cdot q_h(z)$. The sequential voting process in the experiment is described by a non-linear Pólya urn. It was shown that $q(z)$ has one (two) stable fixed point(s) for $p < p_c (> p_c)$.

If there is only one stable fixed point, $z(t)$ converges to it. In the case of multiple stable fixed points, the stable fixed point to which z converges will be random[13]. By controlling the model parameters, the number of stable fixed points can be changed, which induces a non-equilibrium transition. In an exactly solvable case, where $q(z)$ is a combination of the constant $q_* \in (1/2, 1]$ and the Heaviside function $\theta(z-1/2)$, i.e., $q(z) = (1-p) \cdot q_* + p \cdot \theta(z-1/2)$ with a correlation control parameter $p \in [0, 1]$, $q(z)$ touches the diagonal at $z_t = 1/2$ for $p = p_c = 1 - 1/2q_*$. For $p < p_c$, there is a unique stable state at $z_+ = (1 - p)q_* + p$. For $p > p_c$, there are two stable states at $z_{\pm} = (1 - p)q \pm p$. Because the slope of $q(z)$ in the left neighborhood of z_t is 0, the touchpoint at z_t is unstable, and $z(t)$ converges to the stable fixed point at z_+ for $p = p_c$ [20].

The probability of convergence to a stable fixed point depends strongly on the color of the first ball when there are multiple stable states. If the color is red and $z(1) = 1$ (blue and $z(1) = 0$), the probability of convergence to a larger stable fixed point becomes higher (lower). The difference in the probabilities is given by the limit value c of the normalized correlation function $C(t)$ between the color of the first ball and that of the $t + 1$ -th ball. Furthermore, c plays the role of the order parameter for the phase transition. In the afore-

mentioned exactly solvable model, which we refer to as the "digital" model, $C(t)$ at $p = p_c$ shows a power law dependence on t as $C(t) \propto t^{-\alpha}$ with $\alpha = 1/2$. The order parameter behaves as $c \propto (p - p_c)^\beta$ with $\beta = 1$. In addition, $C(t)$ obeys the scaling form $C(t) \propto t^{-\alpha} g(t/\xi)$ near p_c with a universal function g and correlation length ξ . ξ diverges as $\xi \propto |p - p_c|^{-\nu_{||}}$ with $\nu_{||} = 2$ [21]. The scaling relation $\beta = \nu_{||} \cdot \alpha$ holds as in the absorbing states phase transition [22, 23].

In this work, we use finite-size scaling (FSS) analysis in order to study the asymptotic behavior of the correlation function for generalized Pólya urns. We adopt a logistic-type model $q(z) = (\tanh[J(2z - 1) + h] + 1)/2$ with two parameters J and h . Here, J is the parameter of the strength of the correlation, and h is the parameter of the asymmetry. The motivation for adopting this model was derived from experimental findings [18, 19]. With this choice, there is a threshold value $J_c(h)$, and at $J = J_c(h)$, $q(z)$ becomes tangential to the diagonal at z_t . From the above discussion, the touchpoint at z_t is stable, which differs from the digital model. There are two stable states at z_t and z_+ for $h \neq 0$. If the order parameter c takes a positive value at $J = J_c(h)$, the phase transition becomes discontinuous. For $h = 0$, the touchpoint at $z_t = 1/2$ is the unique stable state. c should be equal to zero and the phase transition becomes continuous. We also clarify the universality class of the continuous transition.

The remainder of the paper is organized as follows. Section II introduces the model. In section III, we discuss the asymptotic behavior of $C(t)$ for $J \neq J_c(h)$ using previous results, and propose the asymptotic form $C(t) \simeq c + c'(\ln t)^{-\alpha'}$ for $J = J_c(h)$. In section IV, we study the FSS relations of the system. Section V is devoted to the FSS study of $C(t)$ for $J = J_c(h)$. We show that $c > 0$ ($c = 0$) and $\alpha' = 1$ ($\alpha' = 1/2$) for $h > 0$ ($h = 0$). The system shows a continuous phase transition for $h = 0$. In section VI, we study the universality class of the continuous transition. We show that $C(t) \propto (\ln t)^{-\alpha'} g(\ln t/\xi)$ with a universal function $g(x)$ and a length scale ξ . We define the critical exponents β and $\nu_{||}$ as $c \propto (J - J_c)^\beta$ and $\xi \propto |J - J_c|^{-\nu_{||}}$, respectively. Using the scaling relation $\beta = \nu_{||} \cdot \alpha'$ with $\nu_{||} = 1$, we obtain $\beta = 1/2$. Section VII provides our summary and further comments. In Appendix A, we derive the explicit form of $g(x)$ for the digital model.

II. MODEL

We define the stochastic process $X(t) \in \{0, 1\}, t \in \{1, 2, \dots, T\}$, where the probability that $X(t)$ takes value of 1 is given by a function $q(z)$ of the proportion $z(t-1)$ of the variables $X(1), \dots, X(t-1)$ that are equal to 1.

$$q(z) \equiv \Pr(X(t) = 1 | z(t-1) = z) = \frac{1}{2} (\tanh [J(2 \cdot z - 1) + h] + 1),$$

$$z(t) = \frac{1}{t} \sum_{s=1}^t X(s) \text{ for } t > 0, \text{ and } z(0) = \frac{1}{2}. \quad (1)$$

The choice of $q(z)$ is arbitrary, and we adopt the above form, which is familiar in the field of physics [24, 25]. The fixed point of $q(z)$ is a solution to $q(z) = z$. Using the mapping $m = 2z - 1$, we obtain the self-consistent equation $m = \tanh(J \cdot m + h)$ for the magnetization m in the mean-field Ising model. Here, we consider only the case for which $J \geq 0$. Because of the symmetry under $(X, h) \leftrightarrow (1 - X, -h)$, we also assume that $h \geq 0$.

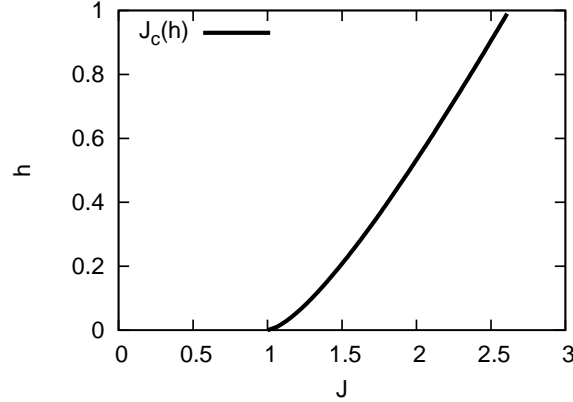


FIG. 1. Plot of $J_c(h)$ in (J, h) .

The number of fixed points for $q(z)$ depends on (J, h) . There is a threshold value $J = J_c(h)$ as a function of h (Fig. 1). For $J < J_c(h)$, there is only one fixed point at $z = z_+$ (Fig.2(a)). With increasing J , $q(z)$ becomes tangential to the diagonal z at z_t for $J = J_c(h)$. For $h > 0$, $z_t \neq z_+$, and both z_t and z_+ are stable (Fig.3(b)). For $h = 0$, $z_t = z_+$, and it is also stable (Fig.3(a)). In both cases, the slope of the curve at z_t is equal to one. For $J > J_c(h)$, there are three fixed points, and we denote them as $z_- < z_u < z_+$; z_{\pm} is stable, and z_u is unstable (Fig.2(b)). We denote the value $q(z_{\pm}), q(z_t)$ as q_{\pm}, q_t and the slope of $q(z)$ at z_{\pm}, z_t as $l_{\pm} \equiv q'(z_{\pm}), l_t = q'(z_t) = 1$. As z_{\pm} is stable and downcrossing, $l_{\pm} < 1$.

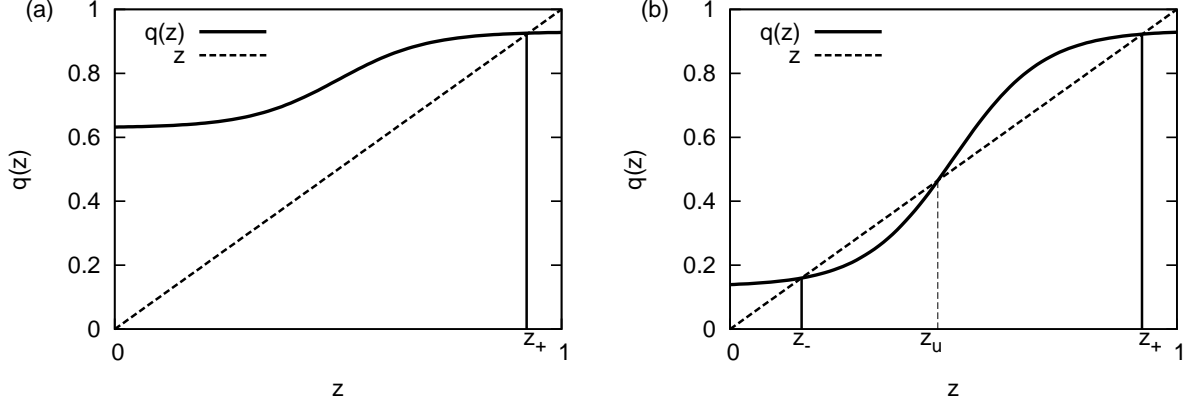


FIG. 2. Plot of $q(z)$ vs. z for $h > 0$. The intersection between $y = q(z)$ and $y = z$ is the fixed point of $q(z)$. (a) $J < J_c(h)$, with one fixed point at $z = z_+$. (b) $J > J_c(h)$, with three fixed points at $z \in \{z_-, z_u, z_+\}$.

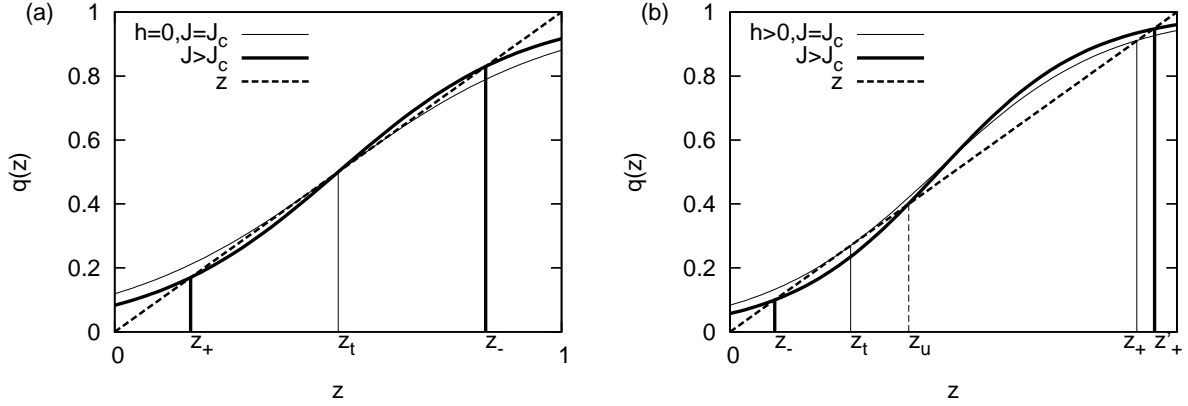


FIG. 3. Plot of $q(z)$ vs. z for $J = J_c(h)$ (thin solid line) and $J > J_c(h)$ (thick solid line) for (a) $h = 0$ and (b) $h > 0$.

We note a crucial difference between $h = 0$ and $h > 0$. For $h = 0$, the touchpoint at $z_t = 1/2$ for $J = J_c(0) = 1$ coincides with the stable fixed point at $z_+ = 1/2$ for $J < J_c(0)$. It splits into the two stable fixed points at $z = z_{\pm}$ for $J > J_c(0)$. (Fig.3(a)). z_{\pm} continuously moves away from z_t and $z_+ - z_- \propto (J - J_c)^{1/2}$ for $|J - J_c| \ll 1$ as in the case of the mean field Ising model. On the other hand, for $h > 0$, the touchpoint z_t appears at a different position from z_+ for $J = J_c(h)$ (Fig.3(b)). As J increases from $J_c(h)$, z_t splits into z_- and z_u . The change from $J < J_c(h)$ to $J > J_c(h)$ is discontinuous. This difference suggests that the phase transition is continuous for $h = 0$ and discontinuous for $h > 0$.

III. ASYMPTOTIC BEHAVIOR OF $C(t)$

In this section, we derive the asymptotic form of the correlation function $C(t)$ using the previous results for $J \neq J_c(h)$. Based on them, we assume the functional form of $C(t)$ for $J = J_c(h)$. $C(t)$ is defined as the covariance between $X(1)$ and $X(t+1)$ divided by the variance of $X(1)$, $\text{Var}(X(1))$:

$$C(t) \equiv \text{Cov}(X(1), X(t+1)) / \text{Var}(X(1)).$$

Through normalization, $C(0) = 1$. $C(t)$ can be expressed as the difference between two conditional probabilities.

$$C(t) = \Pr(X(t+1) = 1 | X(1) = 1) - \Pr(X(t+1) = 1 | X(1) = 0). \quad (2)$$

In general, $C(t)$ is positive for $J > 0$.

A. $C(t)$ for $J \neq J_c(h)$

The asymptotic behavior of $C(t)$ depends on (J, h) . If $J < J_c(h)$, there is one stable fixed point at z_+ and $z(t)$ converges to z_+ through the power-law relation $\text{E}(z(t) - z_+) \propto t^{l_+ - 1}$ [26]. Here, the expectation value $\text{E}(A)$ of a certain quantity A is defined as the ensemble average over the paths of the stochastic process. If $J > J_c(h)$, there is another stable fixed point at z_- . Both z_{\pm} are stable, and $z(t)$ converges to one of the fixed points. The convergence of $z(t)$ to z_{\pm} also exhibits a power-law behavior $\text{E}(z(t) - z_{\pm}) \propto t^{l_{\pm} - 1}$ [27]. We assume that the probability that $z(t)$ converges to one of the z_{\pm} depends on $X(1)$ and we denote this as

$$p_{\pm}(x) \equiv \Pr(z(t) \rightarrow z_{\pm} | X(1) = x).$$

For $J < J_c(h)$, $z(t)$ always converges to z_+ irrespective of the value of $X(1) = x$, and $p_+(x) = 1$ holds. In this case, we set $p_-(x) = 0$. Regarding the asymptotic behavior of the convergence of $z(t) \rightarrow z_{\pm}$, which also depends on $X(1)$, we assume

$$\text{E}(z(t) \rightarrow z_{\pm} | X(1) = x) \simeq W_{\pm}(x) t^{l_{\pm} - 1}$$

We write the dependence of the coefficients $W_{\pm}(x)$ on the value of $X(1)$ explicitly. Using these behaviors and notations, we estimate the asymptotic behavior of $C(t)$ as

$$\begin{aligned}
C(t) &= \Pr(X(t+1) = 1|X(1) = 1) - \Pr(X(t+1) = 1|X(1) = 0) \\
&= E(q(z(t))|X(1) = 1) - E(q(z(t))|X(1) = 0) \\
&= \sum_{x=0}^1 (-1)^{x-1} \{E(q(z(t))|x)\Pr(z(t) \rightarrow z_+|x) + E(q(z(t))|x)\Pr(z(t) \rightarrow z_-|x)\} \\
&\simeq \sum_{x=0}^1 (-1)^{x-1} \{(q_+ + l_+ E(z - z_+|x))p_+(x) + (q_- + l_- E(z - z_-|x))p_-(x)\} \\
&= \sum_{x=0}^1 (-1)^{x-1} \{(q_+ + l_+ W_+(x)t^{l_+-1})p_+(x) + (q_- + l_- W_-(x)t^{l_- -1})p_-(x)\} \\
&= \sum_{x=0}^1 [q_+ p_+(x) + q_- p_-(x) + (l_+ W_+(x)p_+(x)t^{l_+-1} + l_- W_-(x)p_-(x)t^{l_- -1})] (-1)^{x-1}.
\end{aligned} \tag{3}$$

Here, we expand $q(z)$ as

$$q(z) = q(z_{\pm} + l_{\pm} \cdot (z - z_{\pm})) \simeq q_{\pm} + l_{\pm} \cdot (z - z_{\pm}).$$

Given that $p_+(x) + p_-(x) = 1$ for $x = 0, 1$, the limit value $c \equiv \lim_{t \rightarrow \infty} C(t)$ is estimated to be

$$c = (q_+ - q_-)(p_+(1) - p_+(0)). \tag{4}$$

For $J < J_c(h)$, $p_+(x) = 1$ and $c = 0$. As z_- is stable for $J > J_c(h)$, the probability for the convergence of $z(t)$ to z_- is positive. It is natural to assume that $p_+(1) > p_+(0)$ and $c > 0$ for $J > J_c(h)$.

The asymptotic behavior of $C(t)$ is governed by the term with the largest value among $\{l_+, l_-\}$ for $J > J_c(h)$. We define l_{max} as

$$l_{max} \equiv \begin{cases} l_+ & , \quad J < J_c(h), \\ \text{Max}\{l_+, l_-\} & , \quad J > J_c(h). \end{cases} \tag{5}$$

We summarize the asymptotic behavior of $C(t)$ as

$$C(t) \simeq c + c' \cdot t^{l-1} \text{ and } l = l_{max}. \quad (6)$$

Here, we write the coefficient of the term proportional to t^{l-1} as c' . If $J > J_c(h)$, the constant term c is the leading term. If $J < J_c(h)$, the power law term $c' \cdot t^{l-1}$ is the leading term. There also exists a sub-leading term to $c' \cdot t^{l-1}$ that we do not write explicitly. One reason for this is that we do not understand the asymptotic behavior. The second reason is that our interest is focused on the value of l .

B. $J = J_c(h)$

On the boundary $J = J_c(h)$, there are two stable points z_+ and z_t for $h > 0$. As z_t is stable, the probability for the convergence of $z(t)$ to z_t is positive. It is natural to assume that $p_+(1) > p_+(0)$ and $c > 0$. If $h = 0$, there is only one stable point at $z_+ = z_t = 1/2$ and $c = 0$. As $l_{max} = l_t = 1$, we anticipate that $|C(t) - c|$ becomes a decreasing function of $\ln t$. One possibility is a power-law behavior of $\ln t$ such as

$$C(t) \simeq c + c' \cdot (\ln t)^{-\alpha'}. \quad (7)$$

In the case of the digital model, $C(t) \propto t^{-\alpha}$ with $\alpha = 1/2$ for $p = p_c$. We denote the power law exponent for $\ln t$ as α' .

We derive α' by a simple heuristic argument. At first, we consider the case of $h = 0$. There is only one stable touchpoint at z_t , and $z(t)$ converges to it. Eq.(3) suggests that the asymptotic behavior of $C(t)$ is governed by $E(z - z_t|x)$ as z_t is the only stable state. As $q(z_t) = z_t$ and $q'(z_t) = 1$ at z_t , $q(z)$ can be approximated in the vicinity of z_t as

$$q(z) = -\delta(z - z_t)^3 + z.$$

Here δ is a positive constant, as z_t is stable (Fig.3a). The time evolution of $E(z - z_t|x)$ is given as

$$E(z(t+1) - z_t|x) - E(z(t) - z_t|x) = \frac{1}{t+1}E(q(z(t)) - z(t)|x) \simeq -\frac{\delta}{t}E((z - z_t)^3|x).$$

Here the denominator $t + 1$ in the middle of the equation comes from the fact that there occurs a $\frac{1}{t+1}$ change in $E(z(t)|x)$ for $X(t + 1) \in \{0, 1\}$. We also assume $E((z(t) - z_t)^3|x) \simeq E(z(t) - z_t|x)^3$ and the equation can be written as

$$\frac{d}{dt}E(z(t) - z_t|x) = -\frac{\delta}{t}E(z(t) - z_t|x)^3.$$

The solution to this shows the next asymptotic behavior

$$E(z - z_t|x) \propto (\ln t)^{-1/2},$$

and we obtain $\alpha' = 1/2$.

Likewise, for $h > 0$, there are two stable states q_+ and q_t . The subleading term in $C(t)$ is governed by $E(z - z_t|x)$. We can approximate $q(z)$ in the vicinity of z_t to be

$$q(z) = \delta(z - z_t)^2 + z.$$

Here δ is a positive constant (Fig.3b). If $z(t) > z_t$, $z(t)$ moves toward the right-hand direction, on average, and converges to z_+ . We only need to consider the case $z(t) < z_t$ and $z(t)$ converges to z_t . In the case, $E(z(t) - z_t|x)$ obeys the next differential equation.

$$\frac{d}{dt}E(z(t) - z_t|x) = \frac{\delta}{t}E(z(t) - z_t|x)^2.$$

The solution shows the next asymptotic behavior

$$E(z(t) - z_t|x) \propto (\ln t)^{-1},$$

and we obtain $\alpha' = 1$.

C. Numerical check of $C(t) \simeq c + c' \cdot t^{l-1}$

We perform the numerical integration of the master equation of the system and check the asymptotic forms for $C(t)$ numerically. We denote the joint probability function for $\sum_{s=1}^t X(s)$ and $X(1)$ as $P(t, n, x_1) \equiv \Pr(\sum_{s=1}^t X(s) = n, X(1) = x_1)$. For $t = 1$, $P(1, 1, 1) =$

$q(1/2)$ and $P(1, 0, 0) = 1 - q(1/2)$. The other components are equal to zero. The master equation for $P(t, n, x_1)$ is

$$P(t+1, n, x_1) = q((n-1)/t) \cdot P(t, n-1, x_1) + (1 - q(n/t)) \cdot P(t, n, x_1). \quad (8)$$

We impose the boundary conditions $P(t, n, x_1) = 0$ for $n < 0$ or $n > t$. Using $P(t, n, x_1)$ for the case when $t \leq T$, we estimate $C(t)$ for $t < T$.

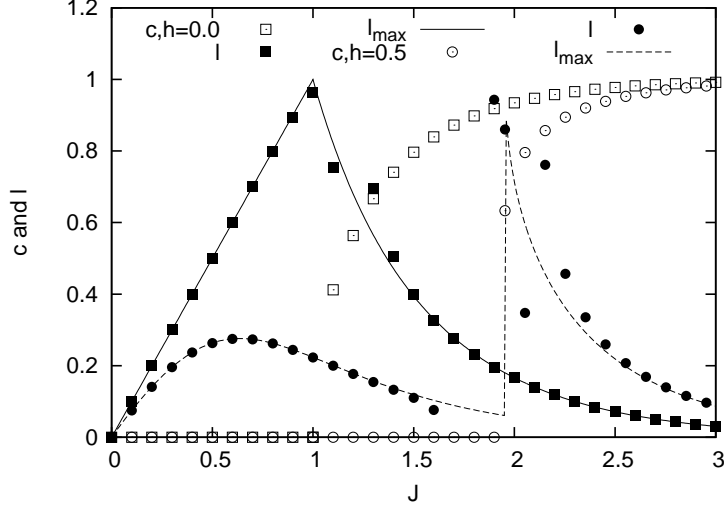


FIG. 4. Plot of c and l in Eqs.(9) and (10) for $h \in \{0.0, 0.5\}$. $\square(\blacksquare)$: $c(l)$ for $h = 0$, and $\circ(\bullet)$: $c(l)$ for $h = 0.5$. The solid (broken) line shows l_{max} for $h = 0.0(0.5)$.

We adopt $h \in \{0.0, 0.5\}$ and $J \in [0, 3]$, and estimate $C(t)$ for $t < T = 4 \cdot 10^5$. The threshold values $J_c(h)$ are $J_c(0) = 1$ and $J_c(0.5) \simeq 1.953$. We assume the asymptotic behavior $C(t) \simeq c + c' \cdot t^{l-1}$ for $J > J_c(0), h = 0$ and $J \geq J_c(h), h > 0$. Using the three values of $C(t)$ at $t_0 = T, t_1 = T/s$, and $t_2 = T/s^2$ with $s = 2$, we solve for c, c' and l in the following manner.

$$\begin{aligned} l &= 1 - \ln_s \frac{C(t_2) - C(t_1)}{C(t_1) - C(t_0)}, \\ c' &= \frac{C(t_1) - C(t_0)}{t_1^{l-1} - t_0^{l-1}}, \\ c &= C(t_0) - a \cdot t_0^{l-1}. \end{aligned} \quad (9)$$

For $J \leq J_c(0), h = 0$ and $J < J_c(h), h > 0$, we assume the asymptotic behavior $C(t) \simeq$

$c' \cdot t^{l-1}$. In this case, we estimate l, c' to be

$$\begin{aligned} l &= 1 - \ln_s C(t_1)/C(t_0), \\ c' &= C(t_0) \cdot t_0^{1-l}. \end{aligned} \tag{10}$$

c and l are plotted using symbols in Fig. 4. We also plotted l_{max} of Eq.(5) with solid and broken lines. The estimation of l obtained using Eqs.(9) and (10) is nearly consistent with l_{max} . However, for $1.2 \leq J \leq 1.5, h = 0.0$ and $2.1 \leq J \leq 2.4, h = 0.5$, large discrepancies are observed in the estimation of l . A possible explanation for these discrepancies is that the system size T is not sufficiently large, and therefore the assumption of the aforementioned asymptotic behavior does not hold. In particular, as t increases, the sign of c' changes at some particular t value, and this negatively affects the estimation of l . We believe that these discrepancies can be removed by increasing the system size T . For $J = J_c(h)$, the aforementioned fitting procedure does not provide accurate results. In the next section, we apply the FSS method and clarify the asymptotic behavior of $C(t)$ for $J = J_c(h)$.

IV. FINITE-SIZE SCALING ANALYSIS

The asymptotic behavior of a system is governed by a temporal length scale, which is referred to as the correlation length ξ . For the definition of ξ , we adopt the second moment correlation length of $C(t)$ [21, 28], which has been adopted in the study of the equilibrium phase transition of spin models [29] and in the percolation theory [30]. We denote the n -th moment of $C(s)$ for the period $s < t$ as $M_n(t) \equiv \sum_{s=0}^{t-1} C(s)s^n$. The variable t in $M_n(t)$ is considered as the time horizon or system size of the stochastic process. The second moment correlation length $\xi(t)$ is defined as $\xi(t) \equiv \sqrt{M_2(t)/M_0(t)}$. The integrated correlation time, also referred to as the relaxation time, $\tau(t)$, is defined as $\tau(t) \equiv M_0(t)$. $\xi(t)$ and $\tau(t)$ have the same dimensions; the length scale in the critical behavior of the system is given by ξ .

A. FSS for $J \neq J_c(h)$

We estimate $M_n(t)$ using the asymptotic behavior of $C(t)$ in Eq.(6).

$$M_n(t) = \sum_{s=0}^t C(s)s^n \simeq \int_0^t C(s)s^n ds = c \frac{t^{n+1}}{n+1} + c' \frac{t^{n+l}}{n+l}.$$

$\xi_t(t) \equiv \xi(t)/t = \sqrt{M_2(t)/M_0(t)t^2}$ is then given as

$$\xi_t(t) \simeq \begin{cases} \sqrt{\frac{l}{l+2}} & , \quad c = 0 \\ \sqrt{\frac{1}{3}} \left(1 + \frac{c'}{2c} \left(\frac{3}{l+2} - \frac{1}{l}\right) t^{l-1}\right) & , \quad c > 0. \end{cases} \quad (11)$$

ξ_t converges to $\sqrt{1/3}$ and $\sqrt{l/(l+2)}$ for $c > 0$ and $c = 0$, respectively.

In the case $c > 0$, we denote the deviation of ξ_t from the limit value $\sqrt{1/3}$ normalized by the limit value as $\Delta\xi_t$.

$$\Delta\xi_t(t) \equiv \frac{\xi_t(t) - \sqrt{1/3}}{\sqrt{1/3}}$$

$\xi_t(t)$ behaves as

$$\xi_t(t) = \sqrt{\frac{1}{3}}(1 + \Delta\xi_t(t)).$$

We also describe $\tau_t(t) \equiv \tau(t)/t$ as

$$\tau_t(t) \simeq c + \frac{c'}{l} t^{l-1}. \quad (12)$$

We express t^{l-1} using $\Delta\xi_t(t)$ for $c > 0$ as

$$\tau_t(t) = c \left(1 + \frac{l+2}{l-1} \Delta\xi_t(t)\right). \quad (13)$$

τ_t converges to c as $\Delta\xi_t(t)$ converges to zero.

We define the scale transformation of the system as the change in the time horizon of the system $t \rightarrow st$ with the scale factor s . We denote the scaling function for a long-term observable $A(t)$ as f_A , which is defined as

$$\frac{A(st)}{A(t)} = f_A(\xi_t(t)) + \Delta f_A(t).$$

Here, we include the correction to the scaling term as $\Delta f_A(t)$. $\Delta f_A(t)$ is of the order $t^{-\omega}$ and ω is a correction-to-scaling exponent[28].

When $C(t)$ exhibits power-law behavior, the system is scale invariant [21]. Furthermore, $\lim_{t \rightarrow \infty} \xi_t(t)$ is constant and $f_{\xi_t} = 1$. Δf_{ξ_t} for $c > 0$ is given by

$$\Delta f_{\xi_t} = \frac{\xi_t(st)}{\xi_t(t)} - 1 \simeq (s^{l-1} - 1)\Delta \xi_t.$$

As $\Delta \xi_t \propto t^{l-1}$, $\omega = l - 1$ for ξ_t .

If $c > 0$, $f_{\tau_t} = 1$ as $\lim_{t \rightarrow \infty} \tau_t = c$, then

$$\Delta f_{\tau_t} = \frac{\tau_t(st)}{\tau_t(t)} - 1 \simeq \frac{l+2}{l-1}(s^{l-1} - 1)\Delta \xi_t.$$

and $\omega = l - 1$. If $c = 0$, $\tau_t \propto t^{l-1}$ and

$$\ln_s f_{\tau_t} = \lim_{t \rightarrow \infty} \ln_s \frac{\tau_t(st)}{\tau_t(t)} = l - 1 = \frac{3 - \xi_t^{-2}}{\xi_t^{-2} - 1}. \quad (14)$$

As $l < 1$, under the scale transformation $t \rightarrow st$, $\tau_t(st) = s^{l-1}\tau_t(t) \propto s^{l-1}$. In the limit $s \rightarrow \infty$, $\tau_t(st)$ decreases to zero.

B. FSS for $J = J_c(h)$

We consider and verify Eq.(7) by studying the finite-size scaling relation of the system. We estimate $M_n(t)$ to $t^{n+1}(\ln t)^{-\alpha'-1}$ as

$$\begin{aligned} M_n(t) &= \int^t C(s)s^n ds \simeq c \frac{t^{n+1}}{n+1} + c' \int^t s^n (\ln s)^{-\alpha'} ds \\ &\simeq c \frac{t^{n+1}}{n+1} + c' \frac{t^{n+1}}{n+1} (\ln t)^{-\alpha'} \left(1 + \frac{\alpha'}{n+1} (\ln t)^{-1} \right). \end{aligned}$$

Here, we use the next expansion in powers of $1/\ln t$, which is obtained by partial integration.

$$\begin{aligned}
\int^t s^n (\ln s)^{-\alpha'} ds &= \frac{1}{n+1} t^{n+1} (\ln t)^{-\alpha'} + \frac{\alpha'}{n+1} \int^t s^n (\ln s)^{-\alpha'-1} ds \\
&= \frac{1}{n+1} t^{n+1} (\ln t)^{-\alpha'} + \frac{\alpha'}{(n+1)^2} t^{n+1} (\ln t)^{-\alpha'-1} + \frac{\alpha'(\alpha'+1)}{(n+1)^2} \int^t s^n (\ln s)^{-\alpha'-2} ds \\
&= \frac{1}{n+1} t^{n+1} (\ln t)^{-\alpha'} + \frac{\alpha'}{(n+1)^2} t^{n+1} (\ln t)^{-\alpha'-1} + O(t^{n+1} (\ln t)^{-\alpha'-2}).
\end{aligned}$$

In the following, we omit the parentheses $(,)$ in $(\ln t)^{-x}$ when we write the power of $\ln t$. $\xi_t(t)$ is

$$\xi_t \simeq \begin{cases} \sqrt{\frac{1}{3}} \left(1 - \frac{2\alpha'}{3} \ln t^{-1}\right) & , \quad c = 0 \\ \sqrt{\frac{1}{3}} \left(1 - \frac{c'}{3c} (\ln t^{-\alpha'-1} - \frac{1}{4} \ln t^{-2\alpha'})\right) & , \quad c > 0. \end{cases}$$

ξ_t converges to the same value $\sqrt{1/3}$ in both cases, $c = 0$ and $c > 0$. However, the convergence speeds differ. The coefficients and exponents of the power of $\ln t$ of the sub-leading terms are given as B and β' , respectively.

$$\xi_t \simeq \sqrt{\frac{1}{3}} (1 - B \ln t^{-\beta'}) \equiv \sqrt{\frac{1}{3}} (1 + \Delta \xi_t(t)) \quad (15)$$

Using the second equality, we define $\Delta \xi_t$. $\beta' = 1$ for $c = 0$ and $\beta' = \text{Min}(1 + \alpha', 2\alpha')$ for $c > 0$.

$\tau_t(t)$ is estimated to be

$$\tau_t \simeq c + c' \ln t^{-\alpha'}. \quad (16)$$

As ξ_t converges to $\sqrt{1/3}$, the system is scale-invariant and $f_{\xi_t} = 1$. For $c = 0$, we can use the scaling relation for τ_t in order to estimate α' . Because τ_t is a function of $\ln t$, we consider the exponential scaling transformation $t \rightarrow t^s$ with the scale factor s .

$$\frac{\tau_t(t^s)}{\tau_t(t)} = s^{-\alpha'}. \quad (17)$$

For $c > 0$, as $f_{\tau_t} = 1$, it is necessary to study the finite-size scaling correction for τ_t .

$$\frac{\tau_t(t^s)}{\tau_t(t)} - 1 \simeq \frac{c'}{c} (s^{-\alpha'} - 1) \ln t^{-\alpha'}. \quad (18)$$

We can estimate α' and c'/c using Eq.(18). In addition, we can estimate β' using ξ_t .

$$\frac{\xi_t(t^s)}{\xi_t(t)} - 1 \simeq (s^{-\beta'} - 1)\Delta\xi_t. \quad (19)$$

If $\alpha' = 1$, a convenient extrapolation formula for c is available. As $\Delta\xi_t = -\frac{c'}{4c}(\ln t)^{-2}$, we can express c'/c using $\Delta\xi_t$ and $\ln t$. We obtain the extrapolation formula for c by solving Eq.(16) as

$$c = \frac{\tau_t(t)}{1 - 4\Delta\xi_t(t) \ln t}. \quad (20)$$

V. NUMERICAL STUDIES OF FSS AND $C(t)$ FOR $J = J_c(h)$

We check the assumption $C(t) \simeq c + c' \ln t^{-\alpha'}$ by studying finite-size scaling. First, we estimate α' for $h = 0$ using Eq.(17) and the data for $t^s = 3 \times 10^6$ and $s \in [1.0, 1, 1]$. Figure 5(a) shows the plotted results. It is evident that the data lies on the curve $s^{-1/2}$ and $\alpha' = 1/2$.

For $h > 0$, we apply Eq.(18) in order to estimate α' . We estimate $\tau_t(t^s)/\tau_t(t) - 1$ for $s = 1.01, 1.001$ and divide it by $s^{-\alpha'} - 1$ using the data for $h \in \{0.1, 0.3, 0.5\}$ and $t^s \leq 5 \times 10^6$. We choose α' so that two data sets with different s lie on the same curve as a function of $1/\ln t$. Figure 5(b) shows the double lnarithmic plot of the obtained results. We choose $\alpha' = 1$ and two data sets for each h that lies on the same curve. If the curve obeys Eq.(18), the slope should be equal to 1 and then, we can estimate c'/c by fitting with $c'/c \ln t$. However, even for $t^s = 5 \times 10^6$, the slope of the curve is not equal to one for $h = 0.1$. We suppose that the system size $t^s = 5 \times 10^6$ is not large enough for Eq.(18) to hold in this case.

In order to verify that $\alpha' = 1$ for $h > 0$, we use Eq.(19). As $\beta' = \text{Min}(1 + \alpha', 2\alpha')$, $\beta' = 2$ for $\alpha' = 1$. We use the estimate of $\xi_t(t^s)/\xi_t(t) - 1$ with the same data set and $s = 1.01, 1.001$. We divide it by $s^{-2} - 1$. Figure 5(c) shows the plotted results. The two data sets for each h lie on the same curve; this agrees with our estimation $\beta' = 2$. Furthermore, as t becomes large, the data set converges to $\Delta\xi$. These results are consistent with Eq.(19) and confirm that $\alpha' = 1$.

We estimate the fitting parameters c, c' using the numerical results of $C(t)$ for $t \leq 5 \times 10^6$. After c is subtracted from $C(t)$, $C(t) - c$ behaves as $c'(\ln t)^{-1}$ for $c > 0$. Figure 6 shows a double lnarithmic plot of $C(t) - c$ vs. $\ln t$ for $J = J_c(h)$. It is difficult to verify the power law

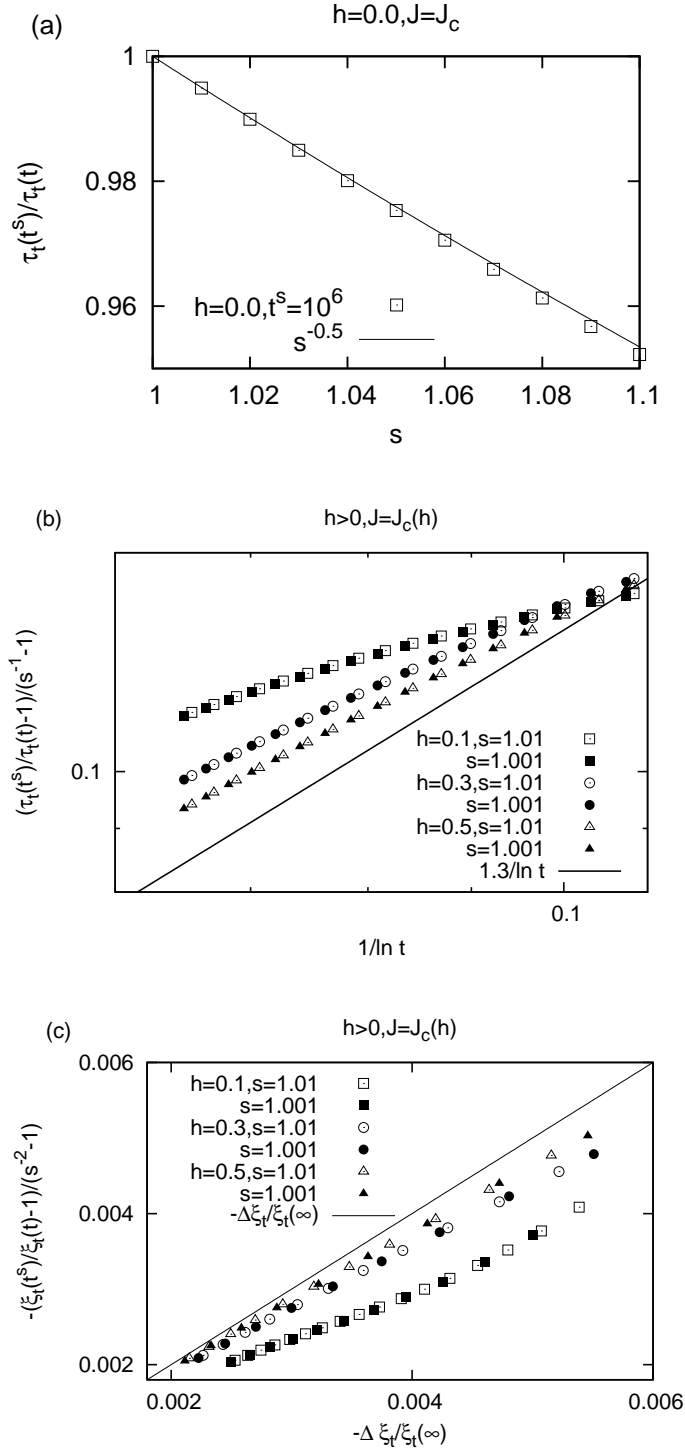


FIG. 5. (a) Plots of $\tau_t(t^s)/\tau_t(t)$ vs. s . (b) Plots of $(\tau_t(t^s)/\tau_t(t) - 1)/(s^{-1} - 1)$ vs. $1/\ln t$. (c) Plots of $-(\xi_t(t^s)/\xi_t(t) - 1)/(s^{-2} - 1)$ vs. $-\Delta \xi_t(t)$. $t < T = 5 \times 10^6 (3 \times 10^6)$ for $h > 0 (h = 0)$

dependence of $C(t) - c$ on $\ln t$ using the narrow range of $\ln t$. The data lies on the straight lines.

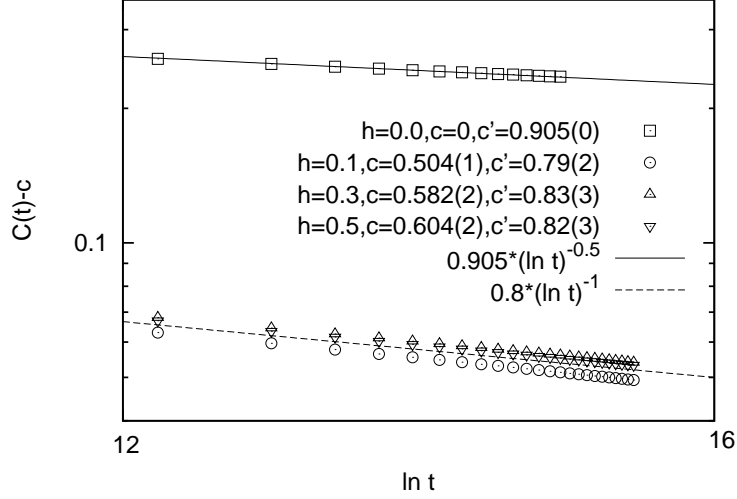


FIG. 6. Plots of $C(t) - c$ vs. $\ln t$ for $J = J_c(h)$ and $h \in \{0.0, 0.1, 0.3, 0.5\}$. $t < T = 5 \times 10^6 (3 \times 10^6)$ for $h > 0 (h = 0)$. For $h = 0.0$, we plot the fitted results using $C(t) = c' \ln t^{-1/2}$ with a fitting parameter of c' . For $h > 0.0$, we plot the fitted results using $C(t) = c + c' \ln t^{-1}$ with two fitting parameters c, c' .

A. Extrapolation of c

We now estimate the limit value $c = \lim_{t \rightarrow \infty} C(t)$ for $J = J_c(h)$. A simple method is to use the fitted result with the assumption that $C(t) = c + c' \ln t^{-1}$. Another method is to use Eq.(20). We summarize the results of these methods in Table I.

TABLE I. The columns in the table denote the following: an estimation of c for $h \in \{0.1, 0.3, 0.5\}$ and $J = J_c(h)$. h in the first column; $C(T - 1)$ in the second column; the estimate by fitting in the third column; $\tau_t(T)$ in the forth column; the estimate using Eq.(20) in the fifth column. $T = 5 \times 10^6$.

h	$C(T - 1)$	c (Fitted)	$\tau_t(T)$	c (Extrapolated)
0.1	0.558	0.504(1)	0.560	0.514
0.3	0.638	0.582(2)	0.640	0.593
0.5	0.659	0.604(2)	0.661	0.615

Both $C(T - 1)$ and $\tau_t(T)$ provide slightly larger estimates of c than the fitting and extrapolation methods. The fitted and extrapolated values are approximately 10% smaller

than the estimates using $C(T-1)$ and $\tau_t(T)$ for $T = 5 \times 10^6$. An extremely slow convergence of $C(t)$ to c is observed.

VI. UNIVERSALITY CLASS

The system shows a continuous phase transition for $h = 0$. As we have seen, the analysis does not depend on the precise form of $q(z)$. As far as $q(z)$ has Z_2 -symmetry, $q(1-z) = 1-q(z)$ and $y = q(z)$ are tangential to $y = z$ at $z_t = 1/2$, we can assume a similar continuous phase transition. In order to discuss the universality class of the phase transition, we compare the scaling properties of $C(t)$ for two models. One model is the logistic model which adopts the $q(z)$ in Eq.(1). For $h = 0$, $J_c(0) = 1$. Another model adopts the next $q_r(z)$ with three parameters $r, p \in [0, 1], q_* \in (1/2, 1]$ [?].

$$\begin{aligned} q_r(z) &= (1-p) \cdot q_* + p \cdot \pi_r(z) \\ \pi_r(z) &= \sum_{s=(r+1)/2}^r {}_r C_s \cdot z^s (1-z)^{r-s} \end{aligned} \quad (21)$$

Here ${}_r C_s$ is the binomial coefficient and r is a odd number greater than three, $r \in \{3, 5, 7, \dots\}$. In the limit $r \rightarrow \infty$, $q_r(z)$ reduces to that of the digital model, $(1-p) \cdot q_* + p \cdot \theta(z - 1/2)$. This model corresponds to the mean-field approximation of the model, where $X(t)$ chooses the majority of r randomly chosen previous variables with a probability of p . For $q_* = 1/2$, $q_r(z)$ has Z_2 -symmetry and the threshold value $p_c(r)$ is determined by the condition $1 = q'_r(z_t = 1/2) = p_c(r) \cdot \pi'_r(1/2)$. p_c is explicitly given as

$$p_c(r) = \frac{[(r-1)/2!]^2 2^{r-1}}{r!}.$$

$p_c(r)$ is a decreasing function of r and $\lim_{r \rightarrow \infty} p_c(r) = 0$, which is compatible with $p_c = 1 - 1/2q_* = 0$ of the digital model with $q_* = 1/2$.

At $J = J_c(0)$, $C(t)$ obeys a power-law of $\ln t$ as $C(t) \simeq c' \ln t^{-\alpha'}$ with $\alpha' = 1/2$ for the former model. Below $J_c(0) = 1$, $C(t) \propto t^{l-1}$ with $l = l_+ = J$. We set $\Delta J = J_c - J = 1 - J$. The expression for the exponent of $C(t) \propto t^{1-l}$ is given by

$$1 - l = \Delta J \quad , \quad J < J_c(0) = 1.$$

For $J > 1$, $C(t) - c \propto t^{l-1}$ with $l = l_+ = l_- = q'(z_+)$. As in the case of the estimation of the critical exponents for the mean-field Ising model [24], we solve $z_+ = q(z_+)$ with the assumption $\Delta J \equiv J - 1 \ll 1$. We obtain $z_+ - 1 = \sqrt{3\Delta J}$ and estimate l as

$$1 - l = \frac{1}{2}\Delta J \quad , \quad J > J_c(0) = 1.$$

As J approaches $J_c(0)$ from below and above of J_c , $1 - l$ approaches 0. At $J = J_c$, $C(t)$ obeys a power-law of $\ln t$. As $t^{-(1-l)} = e^{-(1-l)\ln t}$, we can regard $1/(1-l)$ as the "correlation length" while assuming $C(t)$ as function of $\ln t$. We assume the phenomenological scaling ansatz for $C(t)$ to be

$$C(t) = \ln t^{-\alpha'} g((1-l)\ln t). \quad (22)$$

In the ansatz, $\ln t$ dependence of $C(t)$ is scaled with $1/(1-l)$. $g(x)$ is the universal function and is finite at $x = 0$. For $J = J_c$ and $l = 1$, $C(t) = g(0) \ln t^{-\alpha'}$ with $g(0) = c'$. In the limit $x \rightarrow \infty$, in order to compensate the $\ln t^{-\alpha'}$ term, $g(x)$ should behave as $g(x) \propto x^{\alpha'}$ for $J > J_c(0)$. Then $C(t)$ behaves as $\lim_{t \rightarrow \infty} C(t) \propto (1-l)^{\alpha'} = \Delta J^{\alpha'}$. The critical exponent β for $c \propto \Delta J^\beta$ coincides with α' . The exponent $\nu_{||}$ is defined for the divergence of $1/(1-l)$ as

$$1/(1-l) \propto \Delta J^{-\nu_{||}}.$$

As $(1-l) \propto \Delta J$, we obtain $\nu_{||} = 1$. The scaling relation $\beta = \alpha' \cdot \nu_{||}$ holds.

For the latter model with $q_r(z)$, $l = p \cdot q'_r(z_t = 1/2)$ for $p < p_c(r)$. As $1 = p_c \cdot q'_r(1/2)$ holds, the correlation length $1/(1-l)$ is estimated to be

$$1/(1-l) = \frac{1}{\pi'_r(1/2)(p_c(r) - p)}$$

and diverges as $1/(1-l) \propto \Delta p^{-\nu_{||}}$ with $\nu_{||} = 1$. Here, we define $\Delta p \equiv p_c(r) - p$. For $p > p_c$, we assume $\Delta p = p - p_c(r) \ll 1$ and estimate z_+ by solving $z_+ = q_r(z_+)$ up to $O(\Delta z^3) = O((z_+ - 1/2)^3)$. One may then show that $1-l = q'_r(z_+) \propto \Delta p$, and we obtain $\nu_{||} = 1$. If we assume the scaling form for $C(t)$ to be $C(t) \simeq \ln t^{-\alpha'} \cdot g(\ln t \cdot (1-l))$ and define β as $c \propto \Delta p^\beta$, we obtain $\beta = \alpha' \cdot \nu_{||}$.

If the two models share the same value for α' , this suggests that they are in the same universality class.

A. Numerical calculation of $g(x)$

We estimate the universal function $g(x)$ assumed in Eq.(22) numerically. For the former logistic model with $h = 0$, we estimate that $\alpha' = 1/2$. $J_c(0) = 1$ and we estimate $C(t)$ for $t \leq 4 \times 10^5$ and $2/3 < J < 3/2$. For the latter model with $r = 3$ and $q_* = 1/2$, $p_c(3) = 2/3$. We estimate $C(t)$ for $t \leq 4 \times 10^5$ and $4/9 < p < 1$. Using data for $C(t)$ between $10^4 \leq t \leq 4 \times 10^5$, we determine $g(x)$ to be

$$g(x) = \ln t^{1/2} \cdot C(t) \quad , \quad x = (1 - l) \ln t.$$

$g(x)$ should be smooth near $x = 0$ and $g(0) = c'$. For a sufficiently large J , $c \simeq 1$ and $l = 0$. $g(x)$ should behave as $x^{1/2}$ for sufficiently large x values. For $J < 1$, $g(x)$ should decrease exponentially.

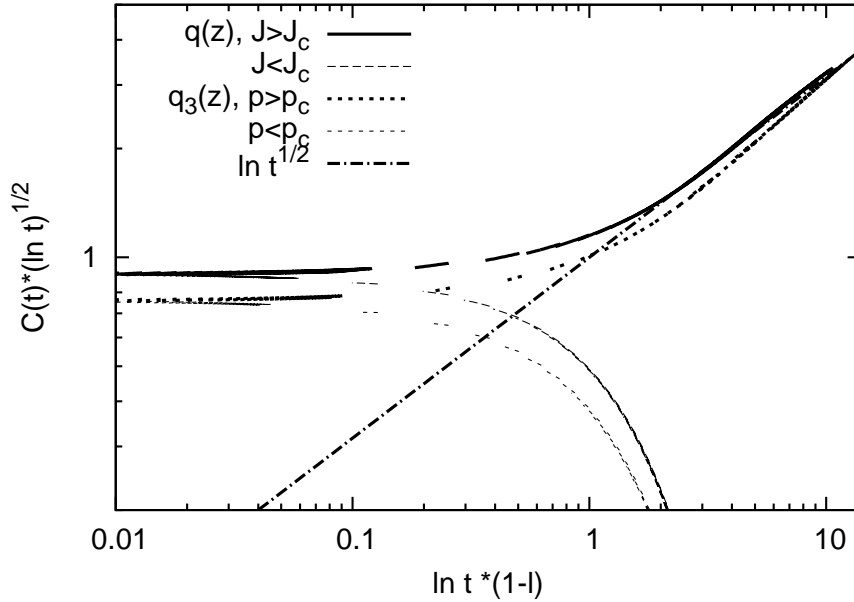


FIG. 7. Plot of $\ln t^{1/2} \cdot C(t)$ vs. $(l - 1) \ln t$.

Figure 7 shows the results of this analysis. The thick continuous and thick dashed lines indicate the results for $J > J_c(0)$ and $p > p_c(3)$, respectively. As can be clearly seen in this figure, the data obtained for different J and t values and for different p and t values lie on two curves, which represent $g(x)$ in the phase with $c > 0$ for both models. For large x , $g(x) \simeq x^{1/2}$. The thin continuous and thin dashed lines indicate the results for $J < J_c(0)$

and $p < p_c(3)$, respectively. The data lie on two curves, which represent $g(x)$ in the phase with $c = 0$ for both models. $g(x)$ can be seen to decay exponentially. The results indicate that the scaling ansatz in Eq.(22) holds with $\alpha' = 1/2$.

VII. SUMMARY AND NOTES

In this study, we analyzed the asymptotic behavior of the normalized correlation function $C(t)$ for a generalized Pólya urn. The probability $q(z)$ of adding a red ball to a specific proportion of red balls z is $q(z) = (\tanh[J(2z - 1) + h] + 1)/2$. There are three domains in (J, h) : $J < J_c(h)$, $J > J_c(h)$, and $J = J_c(h)$, where for $J = J_c(h)$, $q(z)$ becomes tangential to z . The limit value $c = \lim_{t \rightarrow \infty} C(t)$ is the order parameter for the phase transition. If $J < J_c(h)$ ($> J_c(h)$), $c = 0$ ($c > 0$). $C(t) \sim c + a \cdot t^{l-1}$ with $c = 0$ (> 0) for $J < J_c$ ($J > J_c$), and l is the (larger) value of the slope(s) of $q(z)$ at stable fixed point(s). Through FSS analysis, we evaluated the asymptotic behavior of $C(t)$ for $J = J_c(h)$ as $C(t) \simeq c + c' \ln(t)^{-\alpha'}$. For $h = 0$, $c = 0$ and $\alpha' = 0.5$. For $h \neq 0$, $c > 0$ and $\alpha' = 1$. The system shows a continuous phase transition for $h = 0$. $C(t)$ behaves as $C(t) = \ln t^{-\alpha'} g((1 - l) \ln t)$ with a universal function and we numerically estimated $g(x)$. The scaling relation $\beta = \alpha' \nu_{||}$ holds true among the critical exponents with $\alpha' = 1/2$, $\nu_{||} = 1$ and $\beta = 1/2$. We also studied the scaling of $C(t)$ for $q_r(z)$ given in Eq.(21) with $z_* = 1/2$ and $r = 3$. We showed that the scaling ansatz $C(t) = \log t^{-\alpha'} g((1 - l) \log t)$ holds for $\alpha' = 1/2$.

We note several key points and future challenges. The first of these is related to the relationship between the non-equilibrium phase transition studied in this work and equilibrium phase transition of the mean-field Ising (MFI) model for $h = 0$. As is well known, $\beta = 1/2$ for the latter model and both types of phase transitions give the same values for β . A crucial difference lies in the behavior of $C(t)$. In the equilibrium phase transition, the memory of the value of $X(1)$ should disappear for $J < J_c(0)$. However, in the case of the non-equilibrium transition, $C(t)$ decays according to a power-law of t and continues to exist for finite t . Furthermore, for $h > 0$, phase transition does not occur in the equilibrium case and $z(t)$ converges to z_+ . In the non-equilibrium case, the probability for $z(t)$ to converge to z_- is positive for $J > J_c(h)$. In our previous study, we controlled the length of the memory r , and also, $X(t + 1)$ depended only on recent r variables $X(t - r + 1), \dots, X(t)$ [25]. The Pólya urn process corresponds to the case where $r = t$. We have shown that with the

logarithmic increase of $r \propto \ln t$, the non-equilibrium phase transition for $h > 0$ disappears and $z(t)$ always converges to z_+ . We believe that it is possible to understand the relation between the non-equilibrium and equilibrium phase transitions by controlling the increase of r . We assert that if the increase in r is infinitely slowly and the variables are completely equilibrated among the recent r variables, the non-equilibrium phase transition reduces to the equilibrium phase transition.

A problem for the future is related to the derivation of α' and $g(x)$. Our study only provides numerical results and a heuristic derivation of α' ; A more rigorous mathematical treatment appears to be necessary. As the model with $q_r(z)$ shares the same value of $\alpha' = 1/2$ for $r = 3$, and the heuristic derivation of α' only uses the approximate form of $q(z)$ in the vicinity of the touchpoint, the universality class of the continuous phase transition of a generalized Pólya, where $q(z)$ has Z_2 -symmetry and $q(z)$ becomes tangential to the diagonal at $z_t = 1/2$, is described by $\alpha' = 1/2$.

It is also important to verify these results using experimental data. Information cascade experiments could be one possible solution[18, 19]. As the empirically estimated $q(z)$ does not exhibit Z_2 -symmetry at $p = p_c$, the results of this paper suggests that the transition in the experiment is discontinuous. The system size T is severely limited in laboratory experiments. Therefore, web-based experimental systems should be developed in order to study the asymptotic behavior of the system [31].

ACKNOWLEDGMENTS

This work was supported by Grant-in-Aid for Challenging Exploratory Research 25610109.

-
- [1] S. Liu, N. Perra, M. Karsai, and A. Vespignani, Phys. Rev. Lett. **112**, 118702 (2014).
 - [2] J. Fernandez-Gracia, K. Suchecki, J. J. Ramasco, M. S. Miguel, and V. M. Eguíluz, Phys.Rev.Lett. **112**, 158701 (2014).
 - [3] J. González-Avella, V. M. Eguíluz, M. Marsili, F. Vega-Redondo, and M. S. Miguel, PLoS One **6**, e20207 (2011).
 - [4] C. Castellano, S. Fortunato, and V. Loreto, Rev.Mod.Phys. **81**, 591 (2009).
 - [5] P. Curty and M. Marsili, J. Stat. Mech. **2006**, 03013 (2006).

- [6] D. J. Watts, Proc. Natl. Acad. Sci. (USA) **99**, 5766 (2002).
- [7] R. Cont and J. Bouchaud, Macroecon. Dynam. **4**, 170 (2000).
- [8] T. Lux, Econ. J. **105**, 881 (1995).
- [9] G.Pólya, Ann. Inst. Henri Poincaré **1**, 117 (1931).
- [10] M. Hisakado, K. Kitsukawa, and S. Mori, J. Phys. A **39**, 15365 (2006).
- [11] T. Huillet, J.Phys.A **41**, 505005 (2008).
- [12] R. Pemantle, Probab. Surv. **4**, 1 (2007).
- [13] B. Hill, D. Lane, and W. Sudderth, Ann. Prob. **8**, 214 (1980).
- [14] R. Pemantle, Proc. Amer. Math. Soc. **113**, 235 (1991).
- [15] W. B. Arthur, Econ. Jour. **99**, 116 (1989).
- [16] S. Bikhchandani, D. Hirshleifer, and I. Welch, J. Polit. Econ. **100**, 992 (1992).
- [17] L. R. Anderson and C. A. Holt, Amer. Econ. Rev. **87**, 847 (1997).
- [18] S. Mori, M. Hisakado, and T. Takahashi, Phys. Rev. E **86**, 026109 (2012).
- [19] S. Mori, M. Hisakado, and T. Takahashi, J.Phys.Soc.Jpn. **82**, 084004 (2013).
- [20] M. Hisakado and S. Mori, J. Phys. A **44**, 275204 (2011).
- [21] S. Mori and M. Hisakado, J.Phys.Soc.Jpn. **84**, 054001 (2015).
- [22] H. Hinrichsen, Adv.Phys. **49**, 815 (2000).
- [23] G.Ódor, Rev. Mod. Phys. **76**, 663 (2004).
- [24] H. E. Stanley, *Introduction to Phase Transitions and Critical Phenomena* (Oxford University Press, London, 1971).
- [25] M. Hisakado and S. Mori, Physica A **417**, 63 (2015).
- [26] S. Hod and U. Keshet, Phys. Rev. E **70**, 015104 (2004).
- [27] M. Hisakado and S. Mori, J. Phys. A **45**, 345002 (2012).
- [28] S. Caracciolo, R. G. Edwards, S. J. Ferreira, A. Pelissetto, and A. D. Sokal, Phys. Rev. Lett. **74**, 2969 (1995).
- [29] K.Binder, M. Nauenberg, V. Privman, and A. P. Young, Phys. Rev. B **31**, 1498 (1995).
- [30] D. Stauffer and A. Aharony, *Introduction to Percolation Theory* (Taylor&Francis, London, 1991).
- [31] M. J. Salganik, P. S. Dodds, and D. Watts, Science **311**, 854 (2006).

Appendix A: $g(x)$ for the "digital" model

We derive the universal function $g(x)$ for the exactly solvable digital model using the results given in Ref.[21]. We adopt $q(z) = (1 - p) \cdot q_* + p \cdot \theta(z - 1/2)$. The model shows a continuous phase transition at $p = p_c(q_*) = 1 - 1/2q_*$ for $q_* > 1/2$. $C(t)$ behaves as $C(t) \simeq b(q_*)t^{-1/2}$ at $p = p_c(q_*)$. The limit value $c(q_*, p) \equiv \lim_{t \rightarrow \infty} C(t)$ is a continuous function of q_*, p and becomes positive for $p > p_c(q_*)$.

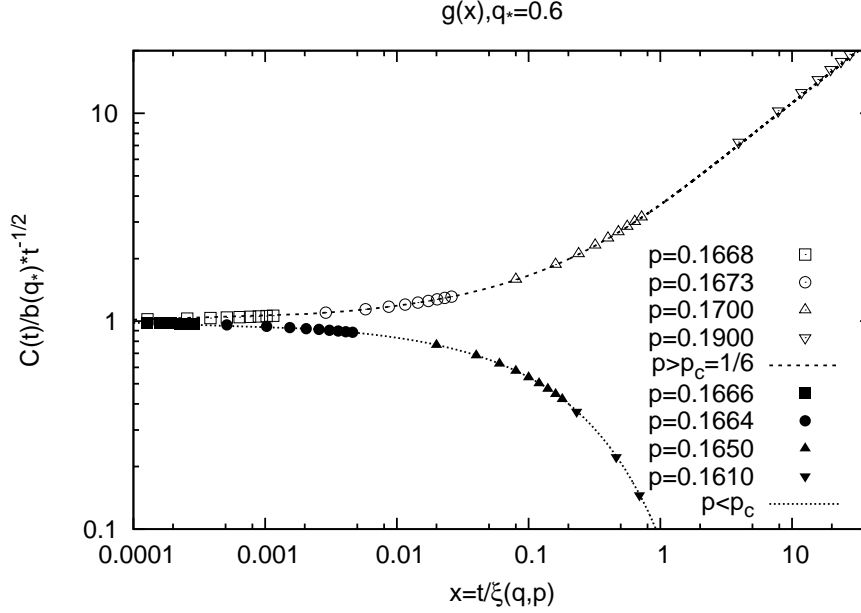


FIG. 8. Plot of $C(t)/b(q_*)t^{-1/2}$ vs. $t/\xi(q_*, p)$ with empty symbols indicating $p > p_c(q_*) = 1/6$ and filled symbols indicating $p < p_c(q_*)$. We adopt $q_* = 0.6$ and $10^4 \leq t \leq 10^5$. The lines show the results of Eq.(A3).

We assume the scaling form for $C(t)$ as

$$C(t) = b(q_*)t^{-1/2}g(t/\xi(q_*, p)). \quad (\text{A1})$$

$b(q_*)$ and $\xi(q_*, p)$ are defined as

$$b(q_*) = \sqrt{\frac{8}{\pi}} \left(\frac{2q_* - 1}{4q_* - 1} \right) \\ \xi(q_*, p)^{-1} = -\ln \sqrt{4(p + (1 - p)(1 - q_*))((1 - p)q_*)} \quad (\text{A2})$$

$g(x)$ is then given as

$$g(x) = \begin{cases} \sqrt{4\pi x} + \frac{x^{1/2}}{2} \int_x^\infty u^{-3/2} e^{-u} du & , \quad p > p_c(q_*), \\ \frac{x^{1/2}}{2} \int_x^\infty u^{-3/2} e^{-u} du & , \quad p < p_c(q_*). \end{cases} \quad (\text{A3})$$

For the derivation of $g(x)$, we use the explicit form of $C(t)$ for $q_* = 1$ given in Ref.[21]. We expand $\xi(q_*, p)$ and $c(q_*, p)$ around $p = p_c(q_*)$ and take the limit $p \rightarrow p_c(q_*)$ by fixing $x = t/\xi(q_*, p)$. For the general $q_* > 1/2$, we estimate $b(q_*)$ using the expressions for $c(q_*, p), \xi(q_*, p)$ and the assumption in Eq.(A1). For sufficiently large x , $g(x) \simeq \sqrt{4\pi x}$. As $\lim_{t \rightarrow \infty} C(t) = c(q, p)$, for $p \simeq p_c(q_*)$, we obtain

$$c(q_*, p) = \sqrt{4\pi} b(q_*) / \sqrt{\xi(q_*, p)}.$$

We can estimate $b(q_*)$ by

$$b(q_*) = \lim_{p \rightarrow p_c(q_*)} \frac{\sqrt{\xi(q_*, p)} c(q_*, p)}{\sqrt{4\pi}}.$$

We have derived $g(x)$ exactly only for $q_* = 1$. We are able to check $g(x)$ for $q_* < 1$. We can estimate $C(t)$ for $t \leq 10^5$ and $q_* = 0.6$ by numerically integrating the master equation for the system. Figure 8 shows the results of this process. The empty symbols indicate the results for $p > p_c(q_*)$. We have adopted the value of p in the vicinity of $p_c(q_*) = 1/6$ and $t \in [10^4, 4 \times 10^5]$. As can be clearly seen, the data obtained for different p and t values lies on the curve of Eq.(A3). The filled symbols indicate the results for $p < p_c(q_*)$. The curve of Eq.(A3) describe the data.